



HAL
open science

Effect of gamma radiation on the photocatalytic properties of Cu doped titania nanoparticles

Lolwa Samet, Katia March, Nathalie Brun, Faouzi Hosni, Odile Stephan,
Radhouane Chtourou

► **To cite this version:**

Lolwa Samet, Katia March, Nathalie Brun, Faouzi Hosni, Odile Stephan, et al.. Effect of gamma radiation on the photocatalytic properties of Cu doped titania nanoparticles. *Materials Research Bulletin*, 2018, 107, pp.1-7. 10.1016/j.materresbull.2018.07.004 . hal-02335615

HAL Id: hal-02335615

<https://hal.science/hal-02335615>

Submitted on 28 Oct 2019

HAL is a multi-disciplinary open access archive for the deposit and dissemination of scientific research documents, whether they are published or not. The documents may come from teaching and research institutions in France or abroad, or from public or private research centers.

L'archive ouverte pluridisciplinaire **HAL**, est destinée au dépôt et à la diffusion de documents scientifiques de niveau recherche, publiés ou non, émanant des établissements d'enseignement et de recherche français ou étrangers, des laboratoires publics ou privés.

Effect of gamma radiation on the photocatalytic properties of Cu doped titania nanoparticles

Lolwa Samet^{1,2,*}, Katia March³, Nathalie Brun³, Faouzi Hosni⁴, Odile Stephan³,
Radhouane Chtourou²

¹*Institut Préparatoires aux Etudes d'Ingénieurs d'El Manar, Université Tunis El Manar, Campus Universitaire Farhat Hached d'El Manar 2092 El Manar, Tunis, Tunisia*

²*Laboratoire de Nanomatériaux et Systèmes pour les Energies Renouvelables, Centre de Recherches et des Technologies de l'Energie, Technopole Borj Cedria, Bp 95, hammamlif 2050, Tunisia*

³*Laboratoire de Physique des Solides, UMR 8502 CNRS - Université Paris-Sud, Bât 510, 91405 Orsay cedex France*

⁴*Laboratoire de Recherche en Energie et Matière pour le Développement des Sciences Nucléaires. Centre National des Sciences et Technologie Nucléaires, 2020 Sidi-Thabet, Tunisia*

*Corresponding author: lolwa.samet@ipeiem.utm.tn

ABSTRACT

The aim of this paper is to study the effect of gamma-rays on structural, physicochemical, optical and photocatalytic performance of TiO₂ nanoparticles doped with different concentrations of copper ranging from 0 to 6 at.%. The powders have been prepared by sol-gel technique and annealed at 400 °C. They were irradiated by gamma-rays with doses varying from 14 to 60 KGy. These investigations confirm the formation of anatase TiO₂ nanoparticles and Cu²⁺ ion substitution for Ti⁴⁺ sites within the TiO₂ structure. This study also shows that, once the TiO₂ structure is saturated with copper, a metallic copper segregation is formed at the crystallite surfaces. After gamma irradiation, samples present a crystalline core and a disordered shell structure as a result of the formation of oxygen vacancies. Such oxygen vacancies at the TiO₂ nanocrystal surface lead to a remarkable enhancement of the photocatalytic activity of Cu-doped TiO₂ catalysts.

Keywords: Titanuim dioxide (TiO₂), Sol-gel, Gamma irradiation, Photocatalysis, EELS, Oxygen vacancy.

1. Introduction

Heterogeneous photocatalysts based on titanium dioxide (TiO_2) have been widely investigated in academic research and extensively involved in industrial applications. However, their photo-conversion efficiency under solar illumination is very limited owing to a too wide intrinsic band gap energy (3.06 eV for rutile and 3.23 eV for anatase). Using sunlight more efficiently to provide energy or to initiate chemical reactions still remains a challenge. Therefore, much effort has been made to extend the light absorption from UV down to the visible region and improve the photoelectrochemical properties of TiO_2 . The most widely adopted strategies are chemical modification by doping (including single metal or non-metal elements, two-element co-doping or self-doping) leading to the extent of the visible light absorption capability in addition to the introduction of cooperative catalysts, that facilitate the separation of photogenerated carriers. Several investigations on doped TiO_2 [1-3] have succeeded in providing some indication about the atomic level details of doping such as the dopant location (e.g. substitutional or interstitial) and discussed the effects of doping on the physical properties and electronic structure of TiO_2 .

Impurity-doped TiO_2 has been attracting a great deal of interest owing to its universal applications especially in different processes for degradation of pollutants and water splitting technologies for photoelectrochemical hydrogen production, see e.g. [4-14]. The presence of non-metal and transition-metal ion dopants in the TiO_2 crystalline matrix significantly influences photoreactivity, charge carrier recombination and interfacial electron-transfer rates.

However, the photoelectrochemical efficiency of doped TiO_2 is still limited by a relative high electron-hole recombination rate. Optimum conditions should be fixed in order to enhance absorption in the visible range and to reduce the charge recombination for an improvement of the photo-response. Indeed, a compromise must be achieved between the light-absorption capability and surface charge transfer rate of the TiO_2 photocatalyst. To avoid

these problems, one approach is to exploit doping or co-doping that involves oxygen vacancies. Previous investigations have revealed that the band gap energy, the electron-hole recombination process as well as the photoelectrical properties of TiO₂ can be effectively tuned by oxygen vacancies [11, 15, 16].

Besides doping, several treatment methods are proposed to achieve visible light absorption for titania catalysts. Some authors studied the effect of plasma treatment on the photocatalytic activity of anatase [16]. They reveal that oxygen vacancies produced by plasma treatment play an important role in the performance activity of treated TiO₂.

Recently, reduction methods (e.g., by high-energy particle bombardment) showed interesting results in producing catalysts with great photocatalytic performance [17-19]. Those methods lead to generate disordered TiO₂ nanophases with simultaneously incorporated oxygen vacancies self-dopants over a few atomic layers at the surface of TiO₂ nanocrystals. In this context, some results, obtained by the application of gamma irradiation treatments on P25 (Degussa) TiO₂ photocatalyst commercial products, showed a surface effect with no significant change on morphology and crystal structure. Optical property investigations revealed an extension of the light absorption from UV down to the visible region, leading to an improvement of the photo-response [18, 19]. These findings have been assigned to trapped electrons in oxygen vacant sites or to Ti³⁺ states formed in the few atomic layers at the surfaces of TiO₂ crystallites. We also note that, according to these articles, both optical band gap value and photocatalytic performance do not vary linearly with the applied gamma doses.

However, this research area is relatively unexplored and many questions deserve to be clarified. In fact, there has been a lack of systematic nanoscale investigation on the nature of the surface modification (structure and composition) in connection with the applied gamma dose. Based on this, we investigated the changes caused by gamma irradiation on anatase

undoped and transition metal incorporated to TiO₂ by a combination of local and global scale characterization techniques.

Doping with copper was chosen. In fact, Cu doped TiO₂ catalysts have recently attracted enormous attention due to their visible light absorption high efficiency. Moreover, the low cost of preparation together with improved catalytic performance, make copper-doped TiO₂ a promising photocatalyst for wide environmental applications. It has been found that the incorporation of copper Cu²⁺ ions into the TiO₂ matrix could be at the origin of such high photocatalytic activity, see e.g. [20-27], by reducing the band gap value down to 1.7 eV as predicted theoretically for a 2 at.% Cu amount [27]. However, the nature of the active copper species (CuO, Cu₂O, metallic Cu, or Cu²⁺ ions in the TiO₂ lattice) that govern photo-reactivity processes is still under debate.

In addition, to further improve photocatalytic performance, it is important to reduce the electron-hole pair recombination and assure a sufficiently long lifetime for this pair which diffuses to the catalyst's surface and initiate a redox reaction. Here, we propose to use Gamma irradiation treatment as a viable way to improve the charge separation. We therefore present a simple and economical method to synthesize efficient TiO₂ photocatalysts reactive to visible-light.

The effect of sunlight illumination on the photocatalytic activity of prepared catalysts was studied by removal of methylene blue (MB) as model of pollutant. To elucidate the factors responsible for the observed effects, initial and gamma irradiated undoped and Cu doped sol-gel TiO₂ products were examined. Changes in absorption properties were evaluated by ultraviolet-visible spectroscopy (UV-vis). Electron paramagnetic resonance (EPR) was used, as a powerful tool to characterize paramagnetic metal ions and defects in the oxide catalysts. The particle size, morphology and crystal structure for each sample type were

determined by transmission electron microscopy (TEM). Microanalysis studies were conducted by electron energy-loss spectroscopy (EELS).

2. Experimental details

2.1. Catalysts Preparation

Pure and Cu²⁺-doped TiO₂ (Cu-TiO₂) powders were prepared via a sol-gel technique [28, 29]. Titanium isopropoxide (Ti(OC₃H₇)₄) was used as TiO₂ precursor, while isopropanol (CH₃CH(OH)-CH₃) and methanol (CH₃OH) were used as solvent and acetic acid (CH₃COOH) as catalyst. Copper chloride (CuCl₂·2H₂O) was used as precursor for Cu²⁺ dopant. The atomic ratio of Cu to Ti were 3 and 6 at.%. Note that undoped TiO₂ samples were prepared as a control in the same way. The obtained millimetric solids were ground in an agate mortar to get fine nanopowders. As-made powders are amorphous. To obtain crystallized samples, these powders were calcined in air at 400 °C during 6 hours. This method allows to obtain powders of high chemical purity.

The synthesized sol-gel powders were exposed to gamma irradiation at ambient temperature of 25 °C (±0.5 °C) using the Tunisian Cobalt-60 irradiator installed in the Tunisian National Center for Nuclear Science and Technology (CNSTN, Technopole of Sidi Thabet, Tunisia). The gamma source consists of eight ⁶⁰Co pencils like-sources arranged and encapsulated in axial symmetry in order to have a better isotropy of gamma photon emission. This source emits gamma photons of 1.2 MeV average energy. In a typical irradiation experiment, 100 mg of each type of TiO₂ powder, undoped and doped with copper, were inserted in eppendorf tubes placed at 15 cm from the gamma source. The applied irradiation doses were 14, 28, and 60 kGy with a dose rate of 80 Gy/min, corresponding respectively to 2h55mn, 5h50mn, 12h30mn time of irradiation. This dose rate was determined by alanine dosimeters irradiated by the facility and returned to aerial for dose rate assessment [30, 31].

2.2. Catalysts characterization

A test of the photocatalytic activity of the synthesized samples were carried outdoors under direct sunlight illumination, during the period of May-June and under clear skies and ambient temperature (25-30 °C) at the university of Tunis el manar (Tunisia, local latitude 36°49'8.29" N, longitude 10°9'56.84" E). The photocatalytic activity was evaluated on the degradation of methylene blue (MB) in aqueous solution. In a typical experiment, the initial concentration of MB aqueous solution was 10 mg/l. The solutions were prepared with deionized water. Prior to irradiation, 60 mg of catalyst was dispersed in 200 ml of prepared MB solution (the amount of catalyst was 0.3 g/L). The solution was magnetically stirred for one hour in darkness to reach adsorption equilibrium. Then, it has been exposed to sunlight illumination by maintaining a continuous magnetic stirring. MB concentration was estimated with a UV-vis spectrophotometer (IC6400). The intensity of the MB absorption peak at about 664 nm was considered to estimate the MB concentration in the solution at the term of the photocatalysis reaction. The efficiency of the degradation process was estimated with the following relation: Degradation % = $(C_0 - C) / C_0$, where C_0 is the initial MB concentration (after one hour in the dark) and C is the MB concentration after certain solar irradiation time.

The optical measurements were performed by diffuse reflection over the 250 to 800 nm wavelength range. The reflection spectrum was measured using a UV-vis-near infrared spectrometer (Lambda-950) equipped with an integrating sphere.

For EPR analysis, the sample was inserted into a standard rectangular cavity in an EMX 71 X-band EPR spectrometer equipped with a 100 kHz magnetic field modulator operating at room temperature.

Samples were investigated in a conventional TEM (TOPCON 002B at 100 keV) for general microstructure characterization. Chemical and electronic properties were investigated by means of EELS performed in two dedicated scanning transmission electron microscopes

(STEM): a probe C_s-corrected Nion Ultra-STEM microscope and a STEM-VG HB501, both equipped with a field emission source operated at 100 keV and coupled to a Gatan EELS spectrometer optically coupled to a high sensitivity (either nitrogen cooled or electron amplifying) CCD camera. Chemical and electronic structure analyses were performed by acquiring collections of EELS spectra in the spectrum-imaging Mode [32]. In such a mode, the focused beam is scanned over a region of interest and a whole spectrum is acquired at each spatial position of the scan. Such a spectrum-image contains typically 10000 spectra. These spectra can be processed individually, usually by removing the background and summing the intensity corresponding to a characteristic edge and thus building elemental maps. However, as this data set contains a lot of redundant information, it is often very useful to process it as a whole and to use multivariate statistical techniques. We used principal component analysis (PCA) as a filtering method for separating meaningful signal components from noise [33].

3. Results and discussion

3.1. Photocatalytic activity results: Outdoor experiments

The photocatalytic efficiency of the TiO₂ catalyst depends on many factors (crystal structure, specific surface area, bulk and surface defects...). Controlling this performance requires the control of the catalyst structural properties. Doping with transition-metal elements affects the lifetime of the charge carriers. In fact, metal doping controls the competition between the electron-hole pair recombination and the transfer rate of the charge carriers from the bulk to the surface, favorable to the increase of photocatalytic activity of TiO₂ catalyst. Therefore the optimization of the doping element concentration is necessary.

The photocatalytic activity evolution of undoped and Cu-TiO₂ initial sol-gel powders and irradiated powders at 60 KGy gamma dose are presented in **Fig. 1**. For non-gamma

irradiated samples, undoped TiO₂ showed the better photocatalytic performance under sunlight illumination as compared to Cu-TiO₂ sol-gel powders. The insertion of Cu at rates of 3 and 6 at.%, leads to a decrease from 40 to 30% (after 5 hours of exposure to sunlight) of the photocatalytic efficiency. Gamma irradiation treatment seems to contribute in favor of enhancing the photocatalytic activity of all prepared TiO₂ catalysts and especially of those at 3 at.% of Cu. The photocatalytic activity of those samples after 60 KGy gamma irradiation is 80% higher than that of the non-irradiated samples.

3.2. Optical and structural investigations

3.2.1. UV-visible diffuse reflectance spectroscopy

The optical properties were determined using diffuse reflectance spectra. The diffuse reflectance data R% was converted to the Kubelka-Munk function F(R) by the equation: $F(R) = \frac{(1 - R)^2}{2R}$ which is proportional to the absorption coefficient [28]. The optical gap value is estimated relying on the Kubelka-Munk method combined with the Tauc relation [34]. The absorption spectra of non-irradiated and gamma irradiated undoped TiO₂ and Cu-TiO₂ powders are represented in **Fig. 2**. For non-irradiated samples, undoped TiO₂ exhibits strong absorption in the UV region and high transparency in the visible one.

Copper incorporation in the TiO₂ lattice leads to a general shift in the UV-visible absorption spectra and an increase of the absorption broad band in the visible range. This typical behavior and this type of electronic transitions is consistent with those obtained in the literature [23-25] and argue in favor of the substitution of Cu²⁺ for Ti⁴⁺ ions that remain in octahedral or pseudo octahedral configuration in the TiO₆ framework. In our case, the most reduced band gap (1.5 eV) was observed for samples synthesized with 3 at.% of Cu. This finding is related to the appearance of new O2p-Cu3d hybridized states at the top of the valence band and the bottom of the conduction band upon Cu²⁺ doping [35]. According to

experimental and theoretical investigations, the substitution of Cu^{2+} for Ti^{4+} in anatase (2 at.% Cu-doped TiO_2) should lead to a decrease in the band gap, down to 1.7 eV, and an increase in the visible light absorption [26, 27]. Indeed, The Cu^{2+} substitution within the crystalline environment of TiO_2 , also leads to an absorption hump extending from 600 to 900 nm that is attributed to d-d transitions [24].

When passing from a copper content of 3 to 6 at.%, the intensity of the absorption band between 400 and 500 nm increases while the broad 600 - 900 nm absorption band decreases (**Fig. 2**). This suggests that the effective doping rate of Cu in the 6 at.% Cu- TiO_2 samples is lower than in 3 at.% Cu- TiO_2 . At a higher incorporation rate of Cu, segregated copper species are observed on the surfaces of the crystallites. More details concerning the effect of doping on structural and optical properties of Cu- TiO_2 sol-gel powders annealed at 400°C have been presented in our previous work [35].

Gamma irradiation treatment significantly affects the absorbance spectra of all studied samples (**Fig. 2**). The absorbance of irradiated samples is always found higher than for non-irradiated ones and an extra peak appears within the wavelength range between 465 nm and 500 nm. No such peak is seen for as prepared sol-gel powders. Also, it is noted that the value of the applied gamma dose did not have much detectable effect on the absorption properties, except for samples prepared with a high Cu level. However, it is known that gamma irradiation leads to the desorption of oxygen from the crystallites surfaces. The extra oxygen vacancies thus formed, may form donor levels in the forbidden band gap of TiO_2 [11, 15] and also affect the electron-hole recombination therefore strongly affecting the photoelectrochemical properties of these catalysts. We will come back to this statement in the nanoscale analysis section.

3.2.2. EPR spectroscopy analysis

An EPR spectroscopy analysis has been performed in order to monitor the involved paramagnetic centers with respect to the Cu incorporation rate and to gamma irradiation dose. This investigation also allows for measuring the oxygen vacancy distribution that occurred during internal incorporation of Cu^{2+} ions in the TiO_2 lattice and gamma treatment. The evolution, as a function of the gamma radiation dose, of the EPR signal of undoped and Cu- TiO_2 samples (3 at.% and 6 at.%) are shown in **Fig. 3(a, b, d)** respectively. The sharp peak observed at $g = 2.001$ is close to the free electron g value ($g = 2.0003$) [24]. In TiO_2 , this value is reported to be due to a single electron trapped in an oxygen vacancy ($V_{\bar{O}}$) [15]. Undoped samples display only this paramagnetic signal whose intensity slightly increases with the dose of gamma irradiation, whereas the line width hardly changes (**Fig. 3(a)**).

After Cu insertion (**Fig. 3(b, d)**), an asymmetric EPR signal shape appears. This EPR signal is present in all Cu- TiO_2 initial and gamma treated samples and corresponds to the presence of Cu^{2+} ($3d^9$) ions in the distorted octahedral coordination of O^{2-} ions [24], which confirms the substitution of Cu^{2+} for Ti^{4+} ions in the TiO_2 structure. These EPR peaks are also broad suggesting that a dipolar interaction is taking place among neighboring Cu^{2+} . The peak-to-peak height (PPH) of Cu^{2+} ion and oxygen vacancy ($V_{\bar{O}}$) signals as a function of the applied gamma dose are shown in **Fig. 3(c)** for undoped and 3 at.% Cu- TiO_2 samples.

For non-irradiated samples, we note that the intensity of the EPR peak assigned to $V_{\bar{O}}$ decreases notably after addition of Cu in the TiO_2 samples [35]. After gamma irradiation such EPR peak increases notably and especially for 3 at.% Cu- TiO_2 , while the 6 at.% Cu- TiO_2 EPR spectrum changes radically. We speculate that a new Cu-rich phase is formed. It has been disclosed that the substitution of Cu^{2+} for Ti^{4+} ions in the TiO_2 lattice leads to the formation of oxygen vacancies inhibiting the formation of Ti^{3+} ions [24, 27]. Indeed, within the detection limits of EPR spectroscopy, no signal corresponding to Ti^{3+} ions was detected. We also note that these oxygen vacancy sites are electron traps. In fact, following the Cu^{2+} doping, the

place occupied by the O^{2-} anion in the regular TiO_2 lattice is taken by one or two free electrons, thus forming a donor level below the conduction band. It is demonstrated that the number of such donor states in both anatase and rutile titania increases with increasing number of oxygen vacancies and can overlap the conduction band [11]. This may explain the great decrease of the TiO_2 band gap upon Cu^{2+} doping. But, in our case the incorporation of Cu^{2+} ions in TiO_2 crystallites is accompanied by a significant decrease in oxygen vacancies or rather in free electrons trapped in these vacant sites. In order to explain these findings, we have performed a nanoscale investigation via EELS analysis.

3.2.3. Nanoscale analysis

Examples of bright Field (BF) images of 3 at.% Cu- TiO_2 annealed at 400°C, obtained during spectro-microscopy measurements, are shown in **Fig. 4(a)**. It can be seen that the average diameter of the crystallites is between 10 and 15 nm and that these crystallites exhibit high crystallinity and well-resolved lattice features throughout the whole polyhedral particles. The application of the PCA technique to EELS performed at sub-nm resolution shows the presence of metallic copper nanoparticles (1-2 nm in diameter) at the surface of the TiO_2 crystallites (see **Fig. 4(b, c)**). From this doping level, the TiO_2 structure begins to be saturated with Cu [35]. The electrons trapped in oxygen vacancies can be transferred to the Cu^{2+} ions segregated on the crystallite surface resulting in metallic Cu formation. This charge transfer can explain the decrease of the $V_{\bar{O}}$ EPR signal PPH in comparison with undoped TiO_2 samples. This decrease in the density of electrons trapped in oxygen vacancies close to the surface may also explain the photocatalytic reactivity reduction of copper doped TiO_2 catalysts.

In addition, in a previous work [35], we have shown by EELS elemental mapping that the insertion of copper in the TiO_2 structure is homogenous within a grain. The amount of Cu inserted (in substitution) in the TiO_2 structure does not exceed 1 at.%. When the copper

solubility limit is exceeded, Cu^{2+} ions are segregated to the grain surfaces in metallic or oxidized form. The total (inserted or segregated) Cu amount varies from a fraction of a percent to about 10% from one grain to another. The same behavior was observed when doping the TiO_2 structure with Co^{2+} ions as reported in a previous article [28].

We now discuss the use of gamma irradiation for the purpose of extra $V_{\bar{O}}$ creation. As shown from the TEM observations (**Fig. 4(d)**) one advantage (at controlled doses) of this method is the little damage at the surface of the crystallites.

For undoped TiO_2 samples, a 27% increase in $V_{\bar{O}}$ was estimated from EPR measurements, which leads to an increase in absorbance in the visible range and an improvement of 10% in photocatalytic efficiency. We have mentioned that 3 at.% Cu- TiO_2 is saturated with less than 1 at.% Cu in substitutional site. In non-gamma irradiated samples, the formation of the metallic copper nanoparticles, which neutralize the free electrons trapped in the $V_{\bar{O}}$ sites created by Cu^{2+} doping, inhibits the photocatalytic reactivity. As shown in **Fig. 3(a, b, c)**, in such relatively less stable structures with larger specific surface areas (25% larger than the undoped TiO_2 samples [28]), the creation of $V_{\bar{O}}$ by gamma irradiation is facilitated. In fact, we note that the Cu^{2+} EPR signal intensity slightly decreases with gamma irradiation dose, whereas the EPR peak assigned to $V_{\bar{O}}$ increases notably. A 400% increase of $V_{\bar{O}}$ is accompanied by a 80% improvement in photocatalytic efficiency. The oxygen vacancy density increase implies a charge carrier density increase on the surface of the crystallites. Moreover, the transfer of the photogenerated electron to the catalyst surfaces can be further facilitated via the Schottky barrier created by the metal-semiconductor interaction at the metallic copper/ TiO_2 interface. Also the excellent electric conductivity of metallic copper has been shown to play an important role in improving photocatalytic activity of Cu- TiO_2 samples.

In order to get some insight about the effect of gamma irradiation at a nanometer scale, anatase 3 at.% Cu-TiO₂ powders irradiated at 60 KGy gamma dose were analysed by high spatially-resolved EELS. For these samples, the typical surface effect (amorphization) is shown on the bright field image of **Fig. 4(d)**. The corresponding EELS spectra for different crystallites in the sample are shown in the energy regions of the TiL_{2,3} (**Fig. 5(a)**) and OK (**Fig. 5(b)**) edges and compared to non-gamma irradiated samples. Both TiL_{2,3} Energy Loss Near Edge Structures (ELNES) in non-gamma irradiated and irradiated samples, are in agreement with Ti⁴⁺ oxidation state in anatase. They exhibit a spin-orbit splitting into 2p^{3/2} (L₃) and 2p^{1/2} (L₂) levels, with a separation of 5 eV. The degree of crystallinity is reflected by the further splitting of the L₂ and L₃ peaks into two peaks due to crystal-field effect: the octahedral coordination of titanium atoms with oxygen splits the Ti3d states into the t_{2g} and e_g symmetries. The right shoulder in the L_{3-eg} peak separated by about 1 eV from the maximum is typical for anatase and has been interpreted as the signature of a structural long-range effect within the crystal [36]. A similar splitting can be observed in the OK edge, which results from the O2p-Ti3d hybridized states of t_{2g} and e_g symmetry [37]. The increase of the oxygen vacancy concentration with applied gamma doses leads to the formation of a defective layer at the TiO₂ crystallite surface. Tan et al. reported similar observations on colored TiO₂ [17]. Indeed, after gamma treatment, TiL_{2,3} and OK ELNES show significant changes. The shape of the TiL₃ edge is very sensitive to local disorder but also to long range order modification induced by the desorption of oxygen. A broadening of the different features in both edges is observed. Such broadening is the result of the superimposition of various crystal field splitting effects and is an indication of the amorphisation of the structure (in the case of TiL_{2,3}, the right shoulder on the L_{3-eg} peak also vanishes as an indication of long range order disappearance). We note that these spectral variations are also compatible with the appearance of a small amount of Ti³⁺.

At high Cu incorporation level (6 at.% Cu-TiO₂) the solubility limits of Cu in the TiO₂ structure is exceeded and the titanium crystallites are mainly encapsulated by a Cu thin layer (**Fig. 4(e)**). EPR investigations confirm that the 6 at.% Cu-TiO₂ non-gamma irradiated crystallites are mainly undoped and that copper species are distributed over the surface of the crystallites, in metallic or Cu₂O forms [35]. Those copper species, by covering the surface of the crystallites, may be at the origin of the photocatalytical efficiency drop by limiting the interaction between the sunlight and the catalyst. According to EPR investigation (**Fig. 3(d)**) and TEM imaging (**Fig. 4(f)**), these copper species are unstable under gamma radiation and transform into Cu-rich nanoparticles, which agglomerate on the surface of the TiO₂ crystallites. TEM images (**Fig. 4(f)**), also show the destructive effect of gamma rays that release the bare surfaces of crystallites. A photocatalytic efficiency improvement of 20% was observed after gamma radiation treatment at 60 KGy.

We now come back to the previous discussion on the peak observed close to 500 nm in the absorption spectra of gamma irradiated samples (**Fig. 2**). Our TEM investigations show a gamma irradiation induced amorphization over thicknesses of a few atomic planes at the surface of the TiO₂ crystallite (section 3. 2. 3). Gamma irradiation also leads to the desorption of oxygen from the TiO₂ crystallite surface. A theoretical study [38] has shown that the formation energy of oxygen vacancies reduces significantly (by a few eV) upon amorphization. Formed oxygen vacancies introduce localized states in the band gap [39] and can be related to the resolution of the extra induced visible band with gamma irradiation.

Other studies [40] showed that the gamma irradiation of borate glasses containing a high TiO₂ content (10%) is responsible for the appearance of small peaks or a shoulder at 540 nm. This specific induced visible peak is ascribed to octahedrally coordinated trivalent titanium (Ti³⁺) ions. Surface Ti⁴⁺ ions can capture released electrons during the irradiation

process and are transformed to Ti^{3+} ions leading to the generation of the low intensity visible peak.

Our EPR investigation does not provide any evidence for the presence of Ti^{3+} ions. However, the local EELS analysis suggests the possible presence of such ions. Therefore, the peak observed close to 500 nm for irradiated samples could also be related to trace Ti^{3+} in the crystallite surface (shell) amorphous layers.

Our photocatalytic experiments show that Cu-TiO₂ with higher oxygen vacancies is more efficient as compared to pure TiO₂, and we confirm that oxygen vacancies play a significant role in both absorption of visible light and photocatalytic efficiency due to the high mobility of their induced charge carriers. Several studies reported a similar synergetic effect in TiO₂ when co-doped with $V_{\bar{O}}$ and nitrogen: photogenerated carrier recombination was shown to be reduced and visible light absorption improved in comparison to N-doped or undoped TiO₂ [41, 42].

4. Conclusion

This study presented a simple and economical method to synthesize efficient visible-light-responsive TiO₂ photocatalysts. Defective pure and Cu doped TiO₂ powders were successfully prepared by combining sol-gel synthesis and gamma treatment. Such samples were characterized by EPR, TEM, EELS and UV spectroscopies. The photocatalytic activity of the obtained powders was evaluated by the photocatalytic degradation of MB. Compared to the non-gamma irradiated TiO₂ powders, it was found that the introduction of defect sites at the TiO₂ catalyst surfaces results in a significant improvement in the photocatalytic efficiency due to the generation of oxygen vacancy electron trapping states. The enhancement of the absorbance of visible light was attributed to both Cu²⁺ substitution and to the presence of extra oxygen vacancies induced by irradiation, which introduce isolated states in the band gap of the TiO₂ catalyst.

This study also showed a close relationship between the gamma irradiation dose and the concentration of defect sites which are related to the destiny of photogenerated electrons and holes. Indeed, the defective sites inhibit the recombination of these electron-hole pairs and thereby increase the concentration of photogenerated carriers at the crystallite surface, leading to an enhancement of the activities of the TiO₂ powders under sunlight irradiation. These results demonstrate the relevance of a strategy exploiting (Cu²⁺, V^{•-}) cooperative effects for promoting the photoelectrochemical properties of TiO₂ powders.

This preparation method by gamma treatment could be potentially used for large-scale production of catalysts with remarkable visible light absorption and photocatalytic activity for wide applications in environmental remediation.

References

- [1] R. Long, N. J. English, Band gap engineering of double-cation-impurity-doped anatase titania for visible-light photocatalysts: a hybrid density functional theory approach, *Phys. Chem. Chem. Phys.* 13 (2011) 13698-13703.
- [2] R. Long, N. J. English, Electronic properties of F/Zr co-doped anatase TiO₂ photocatalysts from GGA + U calculations, *Chem. Phys. Lett.* 498 (2010) 338-344.
- [3] R. Long, N. J. English, Electronic structure of cation-codoped TiO₂ for visible-light photocatalysts applications from hybrid density functional theory calculations, *Appl. Phys. Lett.* 98 (2011) 142103-142105.
- [4] L. Yue, W. Hai-qiang, W. Zhong-biao, Characterization of metal doped titanium dioxide and behaviors on photocatalytic oxidation of nitrogen oxides, *J. Environ. Sci. (China)*. 19 (2007) 1505-1509.

- [5] Q. Hu, J. Huang, G. Li, J. Chen, Z. Zhang, Z. Deng, Y. Jiang, W. Guo, Y. Cao, Effective water splitting using CuO_x/TiO₂ composite films: Role of Cu species and content in hydrogen generation, *Appl. Surf. Sci.* 369 (2016) 201-206 .
- [6] X. H. Xia, L. Lu, A. S. Walton, M. Ward, X. P. Han, R. Brydson, Origin of significant visible-light absorption properties of Mn-doped TiO₂ thin films, *Acta. Mater.* 60 (2012) 1974-1985.
- [7] C. Hsieh, W. Fan, W. Chen, J. Lin, Absorption and visible-light-derived photocatalytic kinetics of organic dye on Co-doped titania nanotubes prepared by hydrothermal synthesis, *Sep. Purif. Technol.* 67 (2009) 312-318.
- [8] M. A Rauf, M. A. Meetani, S. Hisaindee, An overview on the photocatalytic degradation of azo dyes in the presence of TiO₂ doped with selective transition metals, *Desalination.* 276 (2011) 13-27.
- [9] A. L. Castro, M. R. Nunes, M. D. Carvalho, L. P. Ferreira, J. C. Jumas, F. M. Costa, Doped titanium dioxide nanocrystalline powders with high photocatalytic activity, *J. Solid State Chem.* 182 (2009) 1838-1845.
- [10] M. Ni, M. K.H. Leung, D. Y.C. Leung, K. Sumathy, A review and recent developments in photocatalytic water-splitting using TiO₂ for hydrogen production, *Renewable and Sustainable Energy Rev.* 11 (2007) 401-425.
- [11] X. Pan, M. Q. Yang, X. Fu, N. Zhang, Y. J. Xu, Defective TiO₂ with oxygen vacancies: synthesis, properties and photocatalytic applications, *Nanoscale.* 5 (2013) 3601-3614.
- [12] Q. Wang, S. Zhu, Y. Liang, Z. Cui, X. Yang, C. Liang, A. Inoue, One-step synthesis of size-controlled Br-doped TiO₂ nanoparticles with enhanced visible-light photocatalytic activity, *Mater. Res. Bull.* 86 (2017) 248-256.

- [13] X. Tang, Z. Wang, W. Huang, Q. Jing, N. Liu, Construction of N-doped TiO₂/MoS₂ heterojunction with synergistic effect for enhanced visible photodegradation activity, *Mater. Res. Bull.* 105 (2018) 126-132.
- [14] X. Sun, C. Liu, Z. Chen, Y. Ma, The photocatalytic performance of Ta and Rh co-doped TiO₂ tuned by the average dopant valence, *Mater. Res. Bull.* 100 (2018) 153-160.
- [15] Y. Sun, T. Egawa, L. Zhang, X. Yao, Novel method to directly prepare high-surface-area anatase titania nanoparticles with trapped electrons on oxygen vacancies, *J. Mater. Sci. Lett.* 22 (2003) 799-802.
- [16] B. Bharti, S. Kumar, N. H. Lee, R. Kumar, Formation of oxygen vacancies and Ti³⁺ state in TiO₂ thin film and enhanced optical properties by air plasma treatment, *Nature Scientific Reports.* 6 (2016) 32355-32367.
- [17] H. Tan, Z. Zhao, M. Niu, C. Mao, D. Cao, D. Cheng, P. Feng, Z. Sun, A facile and versatile method for preparation of colored TiO₂ with enhanced solar-driven photocatalytic activity, *Nanoscale.* 6 (2014) 10216-10223.
- [18] M. P. Bello Lamo, P. Williams, P. Reece, G. R. Lumpkin, L. R. Sheppard, Study of gamma irradiation effect on commercial TiO₂ photocatalyst, *Appl. Radiat. Isot.* 89 (2014) 25-29.
- [19] R. Kralchevska, M. Milanova, M. Tsvetkov, D. Dimitrov, D. Todorovsky, Influence of gamma-irradiation on the photocatalytic activity of Degussa P25 TiO₂, *J. Mater. Sci.* 47 (2012) 4936-4945.
- [20] I. Ganesh, P. P. Kumar, I. Annapoorna, J. M. Sumliner, M. Ramakrishna, N. Y. Hebalkar, G. Padmanabham, G. Sundararajan, Preparation and characterization of Cu-doped TiO₂ materials for electrochemical, and photocatalytic applications, *Appl. Surf. Sci.* 293 (2014) 229-247.

- [21] W. P. Hudson, M. V. J. R. Carvalho, P. Hammer, C. R. Teodorico, TiO₂-Cu photocatalysts: a study on the long- and short-range chemical environment of the dopant, *J. Mater. Sci.* 48 (2013) 3904-3912.
- [22] B. Xin, P. Wang, D. Ding, J. Liu, Z. Ren, H. Fu, Effect of surface species on Cu-TiO₂ photocatalytic activity, *Appl. Surf. Sci.* 254 (2008) 2569-2574.
- [23] G. Colon, M. Maicu, M. C. Hidalgo, J. A. Navio, Cu-doped TiO₂ systems with improved photocatalytic activity, *Appl. Catal., B.* 67 (2006) 41-51.
- [24] B. Choudhury, M. Dey, A. Choudhury, Defect generation, d-d transition, and band gap reduction in Cu-doped TiO₂ nanoparticles, *Int. Nano Lett.* 3 (2013) 25-33.
- [25] T. Aguilar, J. Navas, R. Alcántara, C. Fernández-Lorenzo, J. J. Gallardo, G. Blanco, J. Martín-Calleja, A route for the synthesis of Cu-doped TiO₂ nanoparticles with a very low band gap, *Chem. Phys. Lett.* 571 (2013) 49-53.
- [26] A. Dashora, N. Patel, D. C. Kothari, B. L. Ahuja, A. Miotello, Formation of an intermediate band in the energy gap of TiO₂ by Cu-N-codoping: first principles study and experimental evidence, *Sol. Energy. Mat. Sol. C.* 125 (2014) 120-126.
- [27] J. Navas, A.S. Coronilla, T. Aguilar, N.C. Hernandez, D. Santos, J.S. Marquez, D. Zorrilla, C. F. Lorenzo, R. Alcantara, J. M. Calleja, Experimental and theoretical study of the electronic properties of Cu-doped anatase TiO₂, *Phys. Chem. Chem. Phys.* 16 (2014) 3835-3845.
- [28] L. Samet, J. Bennasseur, R. Chtourou, K. March, O. Stephan, Heat treatment effect on the physical properties of cobalt doped TiO₂ sol-gel materials, *Mater. Charact.* 85 (2013) 1-12.
- [29] J. Ben Naceur, M. Gaidi, F. Bousbih, R. Mechiakh, R. Chtourou, Annealing effects on microstructural and optical properties of nanostructured-TiO₂ thin films prepared by sol-gel technique, *Curr. Appl. Phys.* 12 (2012) 422-428.

- [30] F. Hosni, K. Farah, H. Kaouach, A. Louati, R. Chtourou, A. H. Hamzaoui, Effect of gamma-irradiation on the Colorimetric properties of epoxy-resin films: potential use in dosimetric application, *Nuclear Instruments and Methods in Physics Research B*. 311 (2013) 1-4.
- [31] F. Hosni, K. Farah, A. Mejri, A. Khayat, R. Chtourou, A. H. Hamzaoui, A study of the fractionation dose on the radiation response of Harwell Red-Perspex PMMA dosimeter, *Nucl. Instrum. Methods Phys. Res. Sect. B*. 290 (2012) 69-71.
- [32] C. Jeanguillaume & C. Colliex, Spectrum-image: the next step in EELS digital acquisition and processing, *Ultramicroscopy*. 198928 (1989) 252-257.
- [33] F. De La Peña, M. H. Berger, J. F. Hochepeid, F. Dynys, O. Stephan, M. Walls, Mapping titanium and tin oxide phases using EELS: An application of independent component analysis, *Ultramicroscopy*. 111(2) (2011) 169-176.
- [34] S. Tandon, J. Gupta, Measurement of forbidden energy gap of semiconductor by diffuse reflectance technique, *Phys. Status. Solidi*. 38 (1970) 363-367.
- [35] L. Samet, K. March, O. Stephan, N. Brun, F. Hosni, F. Bessousa, J. Benasseur, R. Chtourou, Radiocatalytic Cu-incorporated TiO₂ nano-particles for the degradation of organic species under gamma irradiation, *J. Alloys Compd*. 743 (2018) 175-186.
- [36] P. Krüger, Multichannel multiple scattering calculation of L_{2,3}-edge spectra of TiO₂ and SrTiO₃: Importance of multiplet coupling and band structure, *Phys. Rev. B*. 81 (2010) 125121-125126.
- [37] A. Gloter, C. Ewels, P. Umek, D. Arcon, C. Colliex, Electronic structure of titania-based nanotubes investigated by EELS spectroscopy, *Phys. Rev. B: Condens. Matter Mater. Phys.* 80 (2009) 035413-035419.
- [38] H. H. Pham, L. W. Wang, Oxygen Vacancy and hole Conduction in amorphous TiO₂, *Phys. Chem. Chem. Phys.* 17 (2015) 541-550.

- [39] S. Chen, Y. Xiao, Y. Wang, Z. Hu, H. Zhao, W. Xie, A facile approach to prepare black TiO₂ with oxygen vacancy for enhancing photocatalytic activity, *Nanomaterials*. 8 (2018) 245-261.
- [40] A. M. Abdelghany, H.A. El Batal, Effect of TiO₂ doping and gamma ray irradiation on the properties of SrO–B₂O₃ glasses, *J. Non-Cryst. Solids*. 379 (2013) 214-219.
- [41] Y. Chen , X. Cao, B. Gao, B. Lin, A facile approach to synthesize N-doped and oxygen-deficient TiO₂ with high visible-light activity for benzene decomposition, *Mater. Lett.* 94 (2013) 154 -157.
- [42] Y. Chen, X. Cao, B. Lin, B. Gao, Origin of the visible-light photoactivity of NH₃-treated TiO₂: Effect of nitrogen doping and oxygen vacancies, *Appl. Surf. Sci.* 264 (2013) 845-852.

Figures captions:

Fig. 1: Photodegradation efficiency results of MB, under natural sunlight: without catalyst, with initial undoped and Cu-TiO₂ catalyst powders and with undoped and Cu-TiO₂ catalyst powders treated by 60 KGy gamma irradiation dose.

Fig. 2: Diffuse reflectance spectra as a function of gamma irradiation doses of (a) undoped TiO₂, (b) 3 at.% Cu-TiO₂ and (c) 6 at.% Cu-TiO₂.

Fig. 3: EPR spectra of Cu-TiO₂ catalysts annealed at 400°C as a function of gamma irradiation doses: (a) undoped TiO₂, (b) 3 at.% Cu-TiO₂ and (d) 6 at.% Cu-TiO₂. (c) Evolution of the peak-to-peak height of both EPR signatures for divalent copper ions (Cu²⁺) and oxygen vacancies (Vo) as a function of gamma doses for undoped TiO₂ and 3 at.% Cu-TiO₂ catalyst.

Fig. 4: (a) High-resolution Bright Field (BF) image of a 3 at.% Cu-TiO₂ powder annealed at 400°C, (b) Cu elemental map and associated CuL_{2,3} EELS signal extracted after PCA (c) from the reduced area indicated in (a). (d) Bright Field (BF) image of a 3 at.% Cu-TiO₂ powder annealed at 400°C and treated by 28 KGy gamma dose. (e) TEM micrograph of a 6 at.% Cu-TiO₂ powder annealed at 400 °C and (f) after treatment at a 60 KGy gamma dose.

Fig. 5: (a) TiL_{2,3} and (b) OK edge fine structures of 3 at.% Cu-TiO₂ powders annealed at 400°C, before and after 60 KGy gamma treatment.

Fig.1

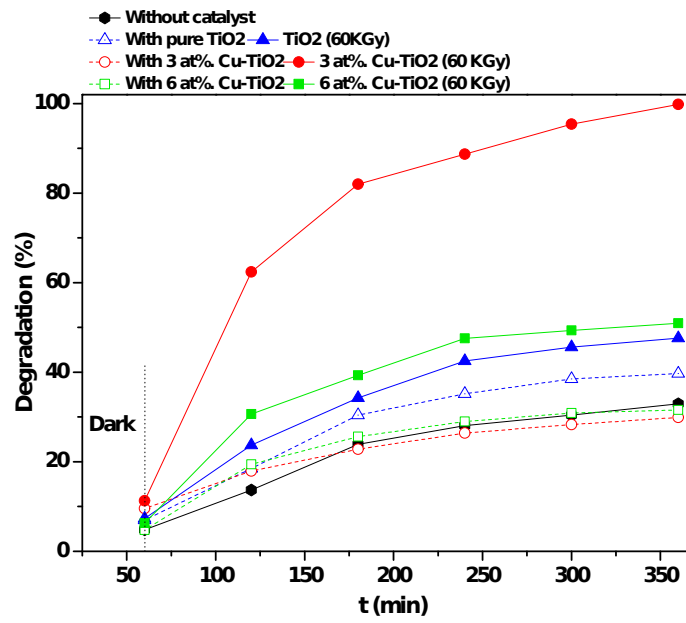


Fig.2

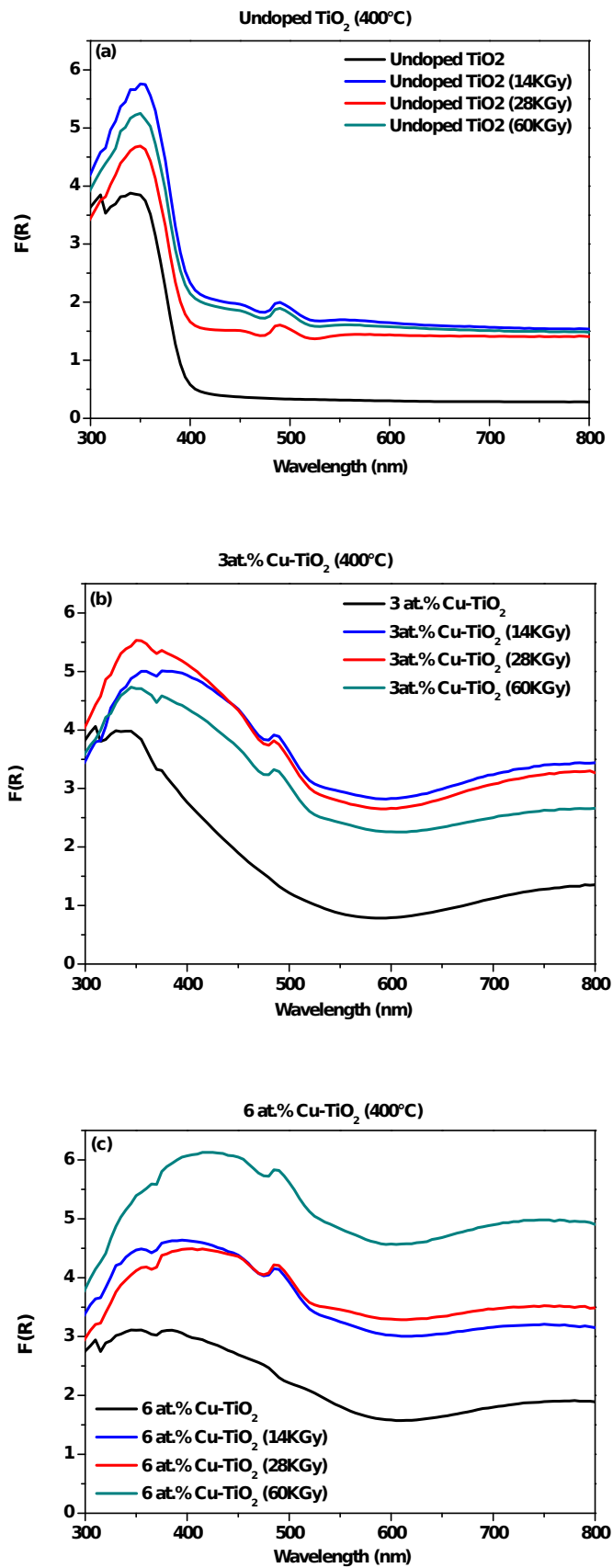


Fig.3

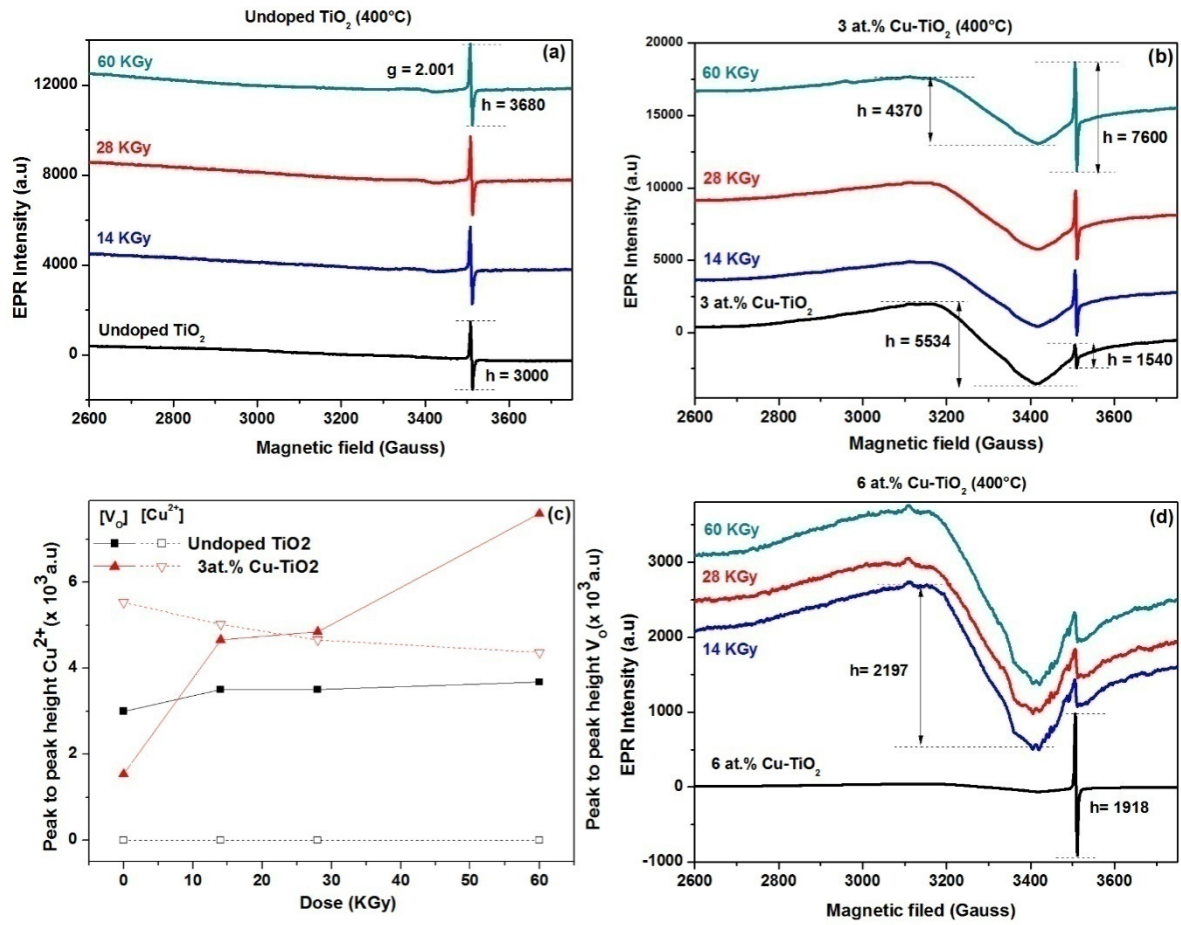


Fig.4

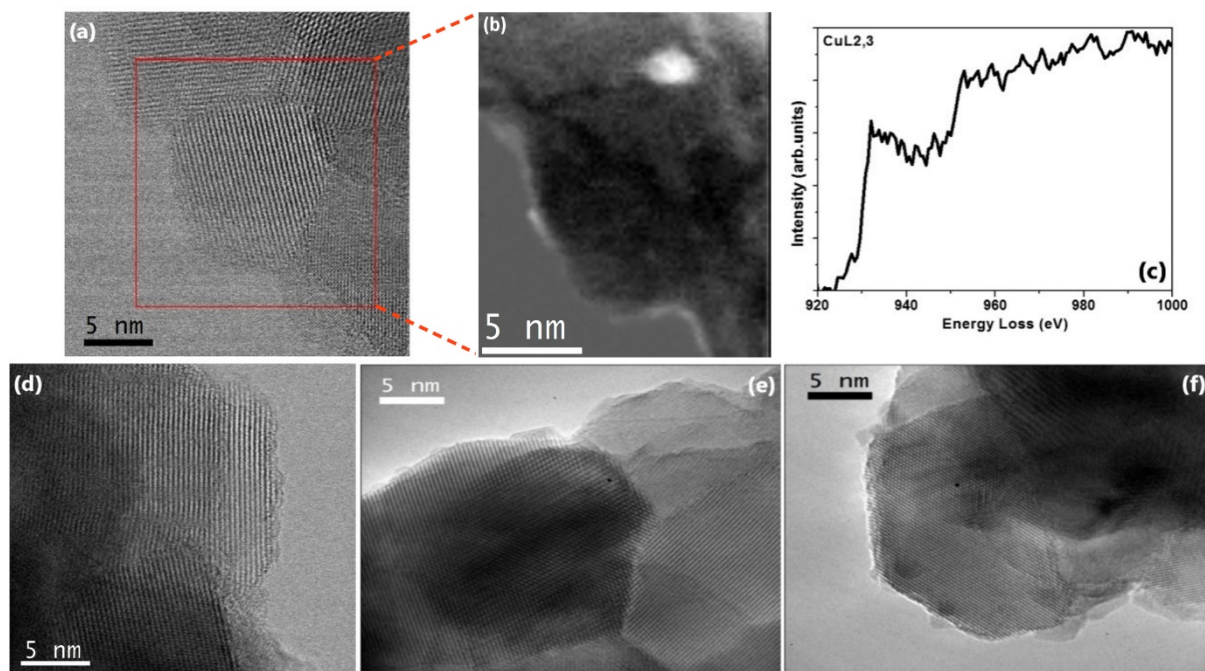


Fig.5

